Plant Physiol. (1997) 115: 1707–1719

Properties of Two Outward-Rectifying Channels in Root Xylem Parenchyma Cells Suggest a Role in K^+ Homeostasis and Long-Distance Signaling[1]

Lars H. Wegner[2] and Albertus H. De Boer*

Faculty of Biology, Department of Genetics, Section of Plant Physiology, Vrije Universiteit Amsterdam, De Boelelaan 1087, 1081HV Amsterdam, The Netherlands

Xylem parenchyma cells (XPCs) control the composition of the transpiration stream in plants and are thought to play a role in long-distance signaling as well. We addressed the regulation, selectivity, and dependence on the apoplastic ion concentrations of two types of outward rectifiers in the plasma membrane of XPCs, to assess the physiological role of these conductances. In whole-cell recordings, the membrane conductance at depolarization was under the control of cytosolic Ca^{2+}: at physiological Ca^{2+} levels (150 nM) the K^+ outward-rectifying conductance (KORC) predominated, whereas at elevated Ca^{2+} levels (5 μM), only the nonselective outward-rectifying conductance (NORC) was active. No such regulatory effect of Ca^{2+} was observed in inside-out experiments. The voltage dependence of whole-cell KORC currents strongly depended on apoplastic K^+ concentration: an increase in apoplastic K^+ resulted in a positive shift of the current-voltage curve, roughly following the shift in Nernst potential of K^+. KORC is impermeable to Na^+, but does translocate Ca^{2+} in addition to K^+. In contrast to KORC, NORC selected poorly among monovalent cations and anions, the relative permeability P_{C+}/P_{A-} being about 1.9. Gating of NORC was largely unaffected by the level of K^+ in the bath. Under all ionic conditions tested, NORC tail currents or single-channel currents reversed close to 0 mV. Using an in vivo xylem-perfusion technique, tetraethylammonium (an inhibitor of KORC) was shown to block K^+ transport to the shoot. These data support the hypothesis that release of K^+ to the xylem sap is mediated by KORC. The molecular properties of these two conductances are discussed in the light of the distinct physiological role of XPCs.

XPCs, the cells surrounding the xylem vessels, are thought to play a key role in salt transport, long-distance signaling, and the ascent of the transpiration stream. In the root, in particular, these cells release mineral nutrients to the xylem that conducts the transpiration stream, forming the main pathway for long-distance transport of salts from the root to the shoot (Clarkson, 1993). Only recently, interest has focused on two other aspects of xylem transport. Based on direct measurements of the pressure relations, the cohesion theory of water movement in the xylem has been questioned (for review, see Zimmermann et al., 1994); in this context, a key role has been postulated for XPCs in building up pressure to drive the ascent of the sap (Canny, 1995) and in maintaining osmotic gradients in the xylem (Zimmermann et al., 1994). Additionally, the xylem has been identified as a pathway for long-distance signaling by hydraulic waves. This signal is thought to be perceived and transduced by XPCs (Malone, 1994).

To understand the mechanisms of these processes, knowledge of the properties of ion channels and conductances in the plasma membrane of XPCs and their functional integration is a prerequisite. So far, little is known about the electrical properties of these cells, partly because they were inaccessible for detailed studies because of their location in the center of the root and shoot and their close connection with other tissues such as the phloem and endodermis. Recently, a method has been designed to isolate protoplasts from the XPCs of nodal roots of barley (*Hordeum vulgare*), allowing the application of the patch-clamp technique to this cell type (Wegner and Raschke, 1994). From whole-cell experiments, two types of outward rectifiers were identified and characterized in a preliminary way. They were found to differ in their voltage dependence, selectivity, kinetics, and pharmacology. One of these rectifiers, the KORC, was proposed to mediate K^+ efflux from XPCs into the xylem vessels, in cooperation with one or several anion conductances. A similar type of KORC has recently been identified in the plasma membrane of stelar cells from maize root (Roberts and Tester, 1995).

In this study we aim to understand the regulation of KORC in the context of K^+ circulation and homeostasis in the whole plant. Using different experimental approaches, xylem loading has been identified as the main site for control of K^+ supply to the shoot. From split-root experiments, Drew and co-workers (Drew and Saker, 1984; Drew et al., 1990) concluded that K^+ transport into the xylem is independent from K^+ uptake by the root, but is regulated by the nutritional status of the plant. The amount of K^+ that is recycled via the phloem (Jeschke et al., 1985) most

[1] This work was supported by the Studienstiftung des Deutschen Volkes (L.H.W.).

[2] Present address: Lehrstuhl für Biotechnologie, Universität Würzburg, Biozentrum am Hubland, D-97074 Würzburg, Germany.

* Corresponding author; e-mail ahdeboer@bio.vu.nl; fax 31–20–444–7155.

Abbreviations: BTP, bis tris propane; E_{K+}, Nernst potential of K^+; E_{rev}, reversal potential; HEDTA, hydroxy EDTA; KORC, K^+ outward-rectifying conductance; NMG, *N*-methylglucamine; NORC, nonselective outward-rectifying conductance; pS, pico-Siemens; TEA, tetraethylammonium; XPC, xylem parenchyma cell.

likely serves as a signal for the demand of the shoot for K^+ (Engels and Marschner, 1992). Properties of the other outward rectifier in XPCs, NORC, are discussed in the light of a possible role in either salt transport to the xylem or in long-distance signaling. The role of cytosolic Ca^{2+} in coordinating the two outward rectifiers is addressed. Our data indicate that the Ca^{2+} status may exert control over the physiological functioning of the cell.

MATERIALS AND METHODS

Plant Cultivation and Protoplast Isolation

Barley (*Hordeum vulgare* cv Apex) was cultivated as described previously (Wegner and Raschke, 1994), and protoplast isolation mainly follows the protocol described in detail in that study. Roots without lateral root formation from the first or second node were collected. The roots had a length of 4 to 6 cm. To optimize the selectivity of the procedure for xylem parenchyma protoplast isolation, stele segments 2 to 3 cm above the root tip were used. These segments were floated in 1 mM $CaCl_2$ after stripping the cortex off by hand, chopping it with a razor blade, and incubating it for 2 h in an enzyme cocktail containing 2% (w/v) cellulase Onozuka R10 (Yakult Honsha, Tokyo, Japan), 0.02% (w/v) pectolyase Y-23 (Seishin Pharmaceutical, Tokyo, Japan), 2% (w/v) BSA, 10 mM sodium ascorbate, 20 mM Glc, 20 mM Suc, and 1 mM $CaCl_2$. The pH was adjusted to 5.5. Mannitol was added to an osmolality of 500 mosmol/kg. After incubation, the suspension was filtered through a 100-μm mesh and rinsed with a wash medium containing 460 mM mannitol, 20 mM Suc, 20 mM Glc, and 1 mM $CaCl_2$. Protoplasts were enriched by two centrifugation steps (10 min at 100*g*) and the pellet of the second step was resuspended in 100 μL of wash medium for patch-clamp experiments. The presence of Suc and Glc during the isolation procedure helped to improve protoplast quality and the seal ratio.

Electrical Recording and Solutions

Conventional patch-clamp procedures were used to monitor currents flowing across the plasma membrane of XPCs (Hamill et al., 1981). Experiments were performed in the whole-cell, inside-out, and outside-out configurations at room temperature. Pipettes were pulled from borosilicate glass capillaries (Kimax 51, Kimble Products, Vineland, NJ). They had a resistance of about 5 to 20 MΩ in symmetrical 100 mM KCl. Voltage clamp was imposed by an amplifier (Axopatch 200A, Axon Instruments, Foster City, CA). Data were stored and pulse protocols were generated on a personal computer (model Vectra 386, Hewlett-Packard) using software from Cambridge Electrical Design (EPC software package, Cambridge, UK) that was connected to the amplifier via an AD/DA converter from Cambridge Electrical Design. For stable electrode potentials at varying Cl− concentrations in the bath, the reference electrode was connected to the bath via a salt bridge containing 1 M KCl in agar.

The composition of the solutions varied among the experiments and is therefore given in the figure legends. Typically, the solution on the cytosolic side of the membrane contained 120 mM potassium glutamate or KCl, and the external solution had 1, 10, 30, or 100 mM KCl. Internal Ca^{2+} was buffered with EGTA (up to 1 μM free Ca^{2+}) or HEDTA (more than 1 μM). The amount of Ca^{2+} to be added to maintain a given free concentration was calculated using the program CALCIUM (Führ et al., 1993). Activities of ions were calculated from concentrations according to the method of Robinson and Stokes (1968). Liquid-junction potentials were determined as described previously (Neher, 1992; Ward and Schroeder, 1994), and were corrected if the value exceeded 2 mV. Data were filtered at 1 kHz and sampled at 3 kHz, if not stated otherwise. Experiments were performed at room temperature (298 K).

Data Analysis

Patch-clamp data were analyzed using Cambridge Electrical Design software. Single-channel traces were evaluated using the program TRANSIT, provided by A.M.J. van Dongen (Department of Pharmacology, Duke University Medical Center, Durham, NC). Tail-current amplitudes were measured 5 to 8 ms after the membrane was clamped to the test potential. The leak was determined by pulse protocols imposed directly before or after a sequence of tail currents was measured. If the leak varied during the experiment, amplitudes of double-exponential fits were taken as tail currents (in the case of NORC, this does not render the correct instantaneous current-voltage relation because NORC was not fully inactivated around the reversal potential). Steady-state current-voltage curves are shown if not stated otherwise.

Sign Convention

Membrane potentials are defined as the voltage on the cytoplasmic side of the membrane with respect to the physiological outside. In inside-out patches, it is the negative value of the technical voltage. Current traces recorded in the inside-out configuration are plotted on an inverted scale, such that downward current deflections denote an inward current in the physiological orientation.

Perfusion Experiments on Intact Seedlings

Barley seedlings grown on 0.5 mM $CaSO_4$ were harvested after 7 d (three to five plants per treatment). Three to five roots per seedling without lateral roots were selected for perfusion, and the other roots were cut off at the base. From the remaining roots, 1 to 2 cm of the tip was removed and about 0.5 cm of the cortex was stripped at the cut end so that a piece of stele was exposed. For perfusion, a setup with two Perspex chambers separated by a wall was used (Fig. 1). The exposed stele was placed into the perfusion medium in the X-compartment (0.5 mM $CaSO_4$, 0.5 mM $MgSO_4$, 2 mM Mes, pH 5.8, and 50 mM TEACl or NMGCl for the control). The remaining part of the roots, up to the

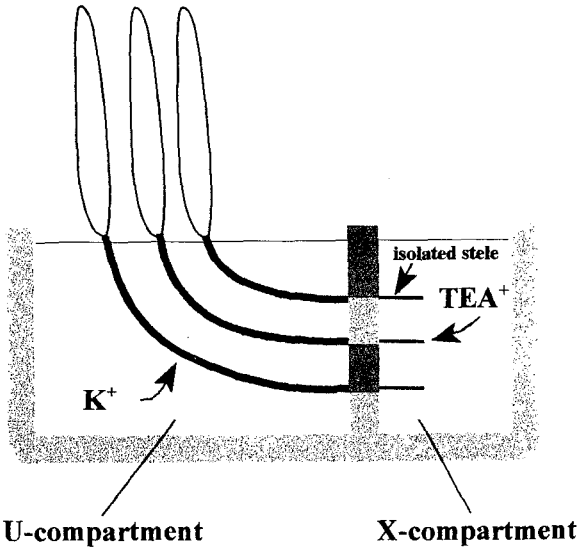

Figure 1. Schematic drawing of the experimental setup used to perfuse the xylem of intact barley seedlings. The Perspex chamber could be divided in two compartments: one compartment in which the exposed xylem could be perfused with, e.g. TEA (the X-compartment), and a second compartment in which the intact roots could take up K^+ from the medium and transfer this to the xylem for transport with the transpiration stream to the shoots (the U-compartment). Roots were sealed into the separating wall with lanolin. Methylene blue, which gives a deep blue color to the solution in the X-compartment, also served to detect possible leakage between the two compartments.

shoot base, were exposed to the uptake medium in the U-compartment.

To prevent ion exchange between the two compartments via the open end of the cortex, roots were pressed into a "sleeve" filled with lanolin. Plants were allowed to draw the perfusion medium into the xylem vessels by transpiration. Uptake was monitored from the flow of 0.02% (w/v) methylene blue through the xylem vessels (root core becomes blue). After 2 to 3 h, unperfused roots were removed, and the U-compartment was filled with 5 mM KNO_3, 0.5 mM $CaSO_4$, 0.5 mM $MgSO_4$, and 2 mM Mes, pH 5.8. Roots were allowed to take up K^+ from the U-compartment for 36 h. Subsequently, the K^+ content in root and shoot was determined by flame photometry. To determine residual K^+, a reference treatment was included identical to the control but without KNO_3 in the U-compartment.

RESULTS

In whole-cell recordings on xylem parenchyma protoplasts, two distinct types of depolarization-activated conductances were identified, which rarely appeared simultaneously in the same protoplast (Wegner and Raschke, 1994). Because of the distinct properties of these channels (with respect to voltage dependence, selectivity, kinetics, and pharmacology), the activation of either channel type could have very different effects on the physiological functioning of xylem parenchyma cells. Therefore, we focused first on the activation mechanism of the two outward rectifiers and studied the effect of fluctuations in cytosolic Ca^{2+}.

The KORC and the NORC: Correlation with the Cytoplasmic Ca^{2+} Concentration

Typical recordings of both outward rectifiers and corresponding current-voltage relations are shown in Figure 2a. Outward currents associated with KORC activated some 20 to 40 mV positive of E_{K+}, were largely K^+ selective, and deactivated slowly (τ about 300 ms) with a single-exponential time course. In contrast, NORC currents were absent or negative in a voltage range between E_{K+} and 0 mV; the current-voltage relation of steady-state and tail currents both intersected the voltage axis close to the origin, and current deactivation was best fitted with a double exponential function (see Wegner and Raschke, 1994, and below). Experiments with different concentrations of free Ca^{2+} in the pipette solution revealed a strong correlation between the frequency at which either KORC or NORC was observed and the cytosolic Ca^{2+} level (Fig. 2b). At low Ca^{2+} KORC predominated, whereas at high Ca^{2+} mostly NORC was active. It should be noted that in about 10 to 50% of the protoplasts (the percentage being variable between different batches), time-dependent outward currents were absent. This indicates that the outward rectifiers may also be subject to other, Ca^{2+}-independent mechanisms of regulation. Data were compiled over a period of about 3 years.

Re-Examination of NORC Voltage Dependence, Selectivity, and Dependence on the Ionic Milieu in the Apoplast

Figure 3a shows whole-cell recordings on a xylem parenchyma protoplast that were performed with 5 μM Ca^{2+} in the pipette solution. The plasma membrane was kept at a holding potential of −101 mV, and positive-going voltage pulses of successively increasing amplitude were imposed at 10-s intervals. Small, time-dependent inward currents were recorded at potentials lower than about 0 mV. Positive potentials gave rise to large outward currents. In many experiments, an instantaneous or quasi-instantaneous component of the outward current was observed in addition to the time-dependent component (Figs. 2a and 3a); it remains unclear if this component is also associated with NORC.

In Figure 3b, the voltage dependence of steady-state currents recorded from one protoplast at 1, 10, and 100 mM KCl in the bath is depicted. Note that currents activated at around −100 mV for all three concentrations. Current density varied among the protoplasts in a voltage-independent manner. Peak inward currents could be in the range of 3 to 6 or 0.1 to 1 μA cm^{-2}. When the cytosolic Ca^{2+} concentration was buffered to 1 μM (Wegner and Raschke, 1994; De Boer and Wegner, 1997), activation of NORC required a depolarization of the membrane beyond 20 to 40 mV, indicating that the voltage dependence of NORC depended on the Ca^{2+} level in the cell. A positive shift in the current-voltage relation of NORC was also observed when the

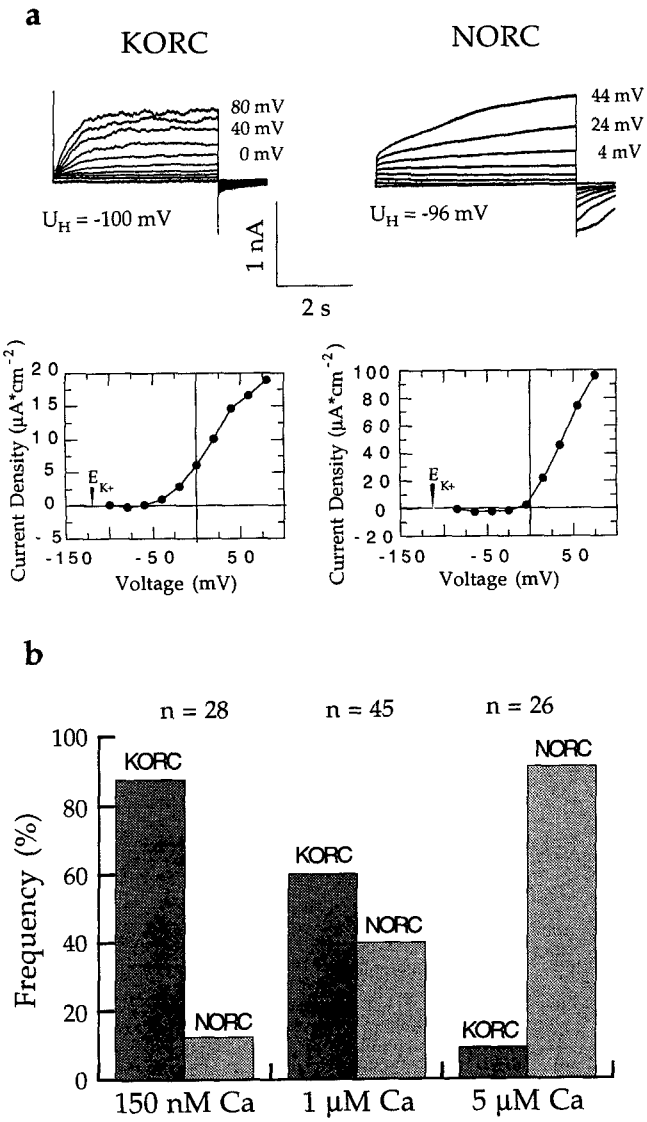

Figure 2. Dependence of the two types of outward rectifiers, KORC and NORC, on the cytosolic Ca^{2+} concentration in whole-cell recordings. a, Typical current traces of KORC and NORC in the whole-cell configuration, and current-voltage plots derived from these experiments (time-dependent currents only), showing the different voltage dependence and kinetic behavior of KORC and NORC. E_{K+} was −116 mV for both experiments. Solutions were: Bath: 1 mM KCl, 2 mM $MgCl_2$, 1 mM $CaCl_2$, 2 mM Hepes (pH 5.8, adjusted with BTP). Pipette for KORC: 120 mM KCl, 10 mM EGTA, 4.42 mM $CaCl_2$, 2.27 mM $MgCl_2$, 2 mM MgATP, 10 mM Tris (pH 7.2, adjusted with Mes; free Ca^{2+} = 150 nM, free Mg^{2+} = 2 mM). Pipette for NORC: 112 mM potassium glutamate, 8 mM KOH, 2 mM HEDTA, 0.099 mM calcium gluconate, 1.67 mM $MgCl_2$, 2 mM MgATP, 10 mM Tris or BTP (pH 7.2, adjusted with Mes; free Ca^{2+} 5 µM, free Mg^{2+} 2 mM). b, Relative frequencies at which KORC and NORC were recorded in whole-cell experiments at different Ca^{2+} concentrations in the pipette medium. The number of protoplasts in which outward currents of either KORC or NORC type were observed is given on top of the bars for each Ca^{2+} concentration separately.

buffer capacity in a Ca^{2+}-free pipette medium was increased by elevating the concentration of EGTA from 0.1 to 5 mM (data not shown). This observation is in agreement with an effect of Ca^{2+} on channel gating.

As reported previously (Wegner and Raschke, 1994), changing the Cl^- gradient across the membrane by substituting Cl^- for glutamate or gluconate did not affect the reversal potential of tail currents. This result had been taken as evidence that NORC currents were exclusively carried by cations, in particular K^+ and Ca^{2+} (but not Mg^{2+}). One obvious way to determine if NORC is a conductance for K^+ and Ca^{2+} is to vary the gradient for these ions and to see if the reversal potential of tail currents is affected. When the Ca^{2+} gradient was abolished by substituting Ca^{2+} in the bath for 2 mM EGTA, a small negative shift in E_{rev} was observed (Fig. 4, a and b). However, the reversal potential remained far from the Nernst potential for K^+, even after removal of Ca^{2+} from the bath (as summarized in Fig. 4c), indicating that ions other than K^+ and Ca^{2+} were also permeable to NORC.

To determine whether the deviation from E_{K+} could be attributable to a proton conductance (the reversal potential for protons being at positive voltages), experiments were repeated with the pH in the bath elevated to 8.0, thus inverting the proton gradient. Changing the pH, however, did not alter the reversal potential of NORC currents significantly. Therefore, we were left with the conclusion that NORC was permeable to both cations and anions, and that it was equally permeable to small anions such as Cl^- and NO^{3-} (data not shown) and to larger anions such as glutamate and gluconate. This explains why no effect on the reversal potential was observed when large anions were exchanged for small anions (Wegner and Raschke, 1994). As can be inferred from Figure 4c, there was a slight preference for cations over anions, because the reversal potential shifted following E_{K+} when the KCl concentration in the bath was increased, but was opposite to the shift in E_{Cl-}. The relative permeability for cations over anions could be estimated using the Goldman equation. It was assumed that the permeability to Cl^- and glutamate was identical, and that the contribution of divalent cations could be neglected. Then, the selectivity for cations over anions, $P_{C+/A-}$, could be calculated according to:

$$P_{C^+/A^-} = \frac{[A]_2 - [A]_1 10^{\Delta E_{rev}/59mV}}{10^{\Delta E_{rev}/59mV}[C]_2 - [C]_1} \quad (1)$$

where $[A]_1$ and $[C]_1$ and $[A]_2$ and $[C]_2$ are the anion and cation activities in the bath at reference conditions and after bath perfusion, respectively, and ΔE_{rev} is the shift in the reversal potential of tail currents. It was calculated that NORC carried monovalent cations about 1.9 times better than anions.

To investigate whether large cations and anions such as organic buffers could also penetrate through NORC, pipette and bath solutions were designed in such a way that the equilibrium potential for both Cl^- and K^+ were identical and nonzero (here, −82 mV). Charge balance was obtained using K-Mes in the pipette and Tris-Cl in the bath. Under these conditions the reversal potential of tail cur-

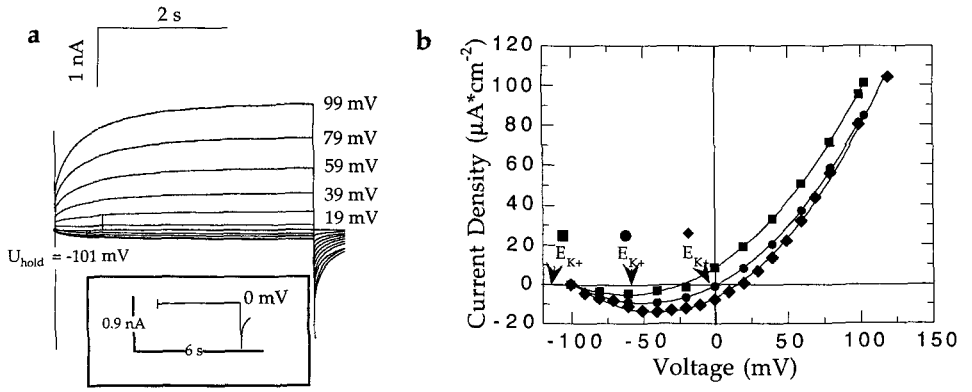

Figure 3. Dependence of NORC on the external K^+ concentration. a, Superimposed traces of NORC currents in a whole-cell experiment. From a holding potential of −101 mV, the membrane was depolarized to potentials ranging from −101 to +99 mV in increments of 20 mV. Between successive sweeps, the membrane was kept at the holding potential for 10 s. For solutions, see Figure 2. Inset, The current trace resulting from a depolarization to 0 mV and successive repolarization to the holding potential is shown separately. Note that no time-dependent current was elicited at the conditioning voltage, but a large tail current appears on repolarization. b, Current-voltage relations of time-dependent currents at 1 (■), 10 (●), and 100 (◆) mM KCl in the bath for the same experiment as shown in a. Solutions were those given in Figure 2 with the exception that KCl in the bath was varied. Nernst potentials for K^+/Cl^- were −116/−17 mV (1 mM KCl), −60/−36 mV (10 mM KCl), and −4/−72 mV (100 mM KCl), respectively.

rents was still close to 0 (E_{rev} = 4 ± 8 mV with 1 mM Ca^{2+} in the bath; n = 4 ± SD) even if Ca^{2+} was removed from the bath (E_{rev} = 5 mV with 2 mM EGTA), indicating that these buffers could penetrate as easily as smaller ions.

Cytosolic Ca^{2+} Does Not Directly Modulate NORC Channels

In inside-out patches, activity of at least one poorly selective ion-channel type could be recorded. Gating manifested itself in stepwise changes of the current level (Fig. 5a). Note the occurrence of substates (see arrowheads) in addition to the main one. For a precise determination of the reversal potential, a protocol of rapid voltage ramps (from 90 to −110 mV in 250 ms) was imposed (Fig. 5b). For leak subtraction, current traces representing the closed state were averaged and subsequently subtracted from recordings of open channels. With 10 mM KCl in the bath and 120 mM potassium glutamate in the pipette, current-voltage relations derived from open-channel ramps intersected the voltage axis at −7 ± 4 mV (n = 11 ± SD from one patch). This value did not correspond to the Nernst potential of

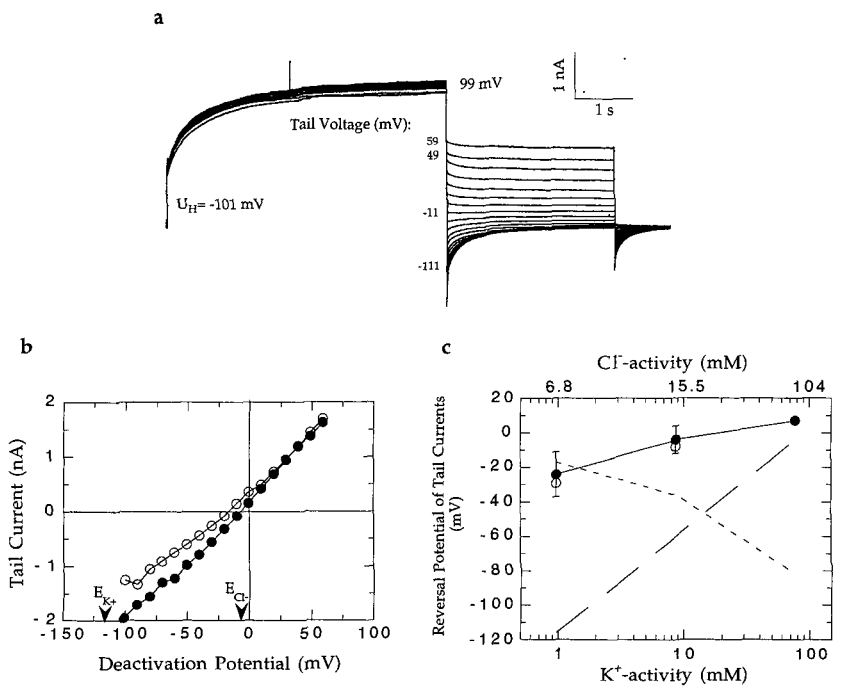

Figure 4. Investigation of NORC selectivity. a, Recordings of a double-pulse experiment on NORC. The cell was depolarized to 99 mV, and subsequently clamped to less-positive potentials in successive sweeps ranging from 59 to −111 mV in steps of 10 mV. For solutions, see Figure 2 (NORC). b, The instantaneous amplitude of tail currents was plotted versus the tail potential to determine the voltage at which tail currents reversed in the presence of 1 mM Ca^{2+} in the bath (●; experiment shown in a) and after replacing Ca^{2+} with 2 mM EGTA (○) by bath perfusion with a solution of otherwise unchanged composition. c, Summary of reversal potential measurements at different K^+ and Cl^- activities and with 1 mM Ca^{2+} in the bath (●) or with Ca^{2+} replaced by 2 mM EGTA (○). Mean values are shown for n = 5 (1 mM K^+, 1 mM $CaCl_2$), n = 2 (1 mM K^+, 2 mM EGTA), n = 5 (10 mM K^+, 1 mM $CaCl_2$), n = 1 (10 mM K^+, 2 mM EGTA), and n = 5 (100 mM KCl, 1 mM $CaCl_2$) experiments with error bars indicating SD. For comparison, the Nernst potentials for K^+ (long-dashed lines) and Cl^- (short-dashed lines) are shown.

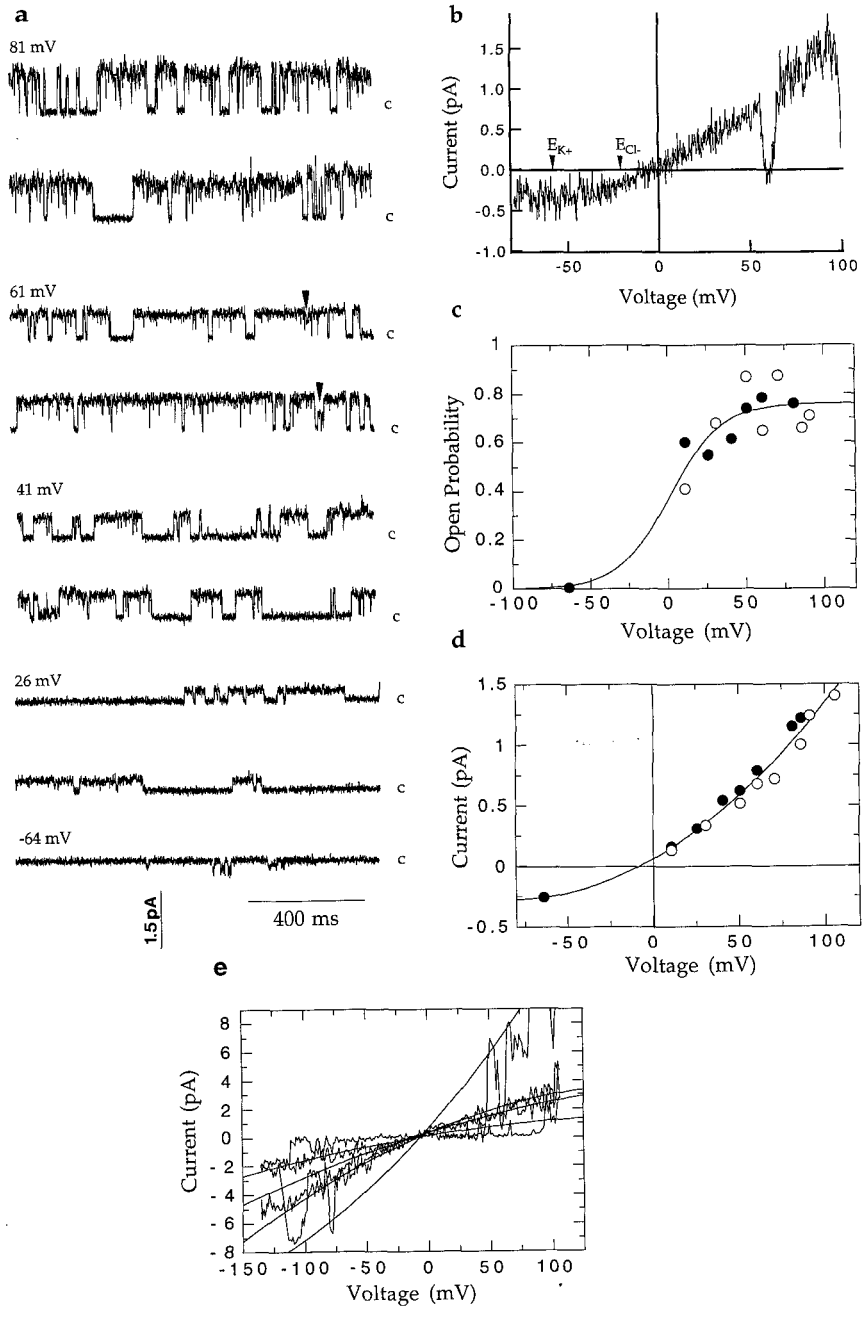

Figure 5. Properties of single NORC channels. a, Current traces recorded on an inside-out patch with NORC-channel activity. Stepwise changes in the current level denote the opening and closing of a single NORC channel. Markers (c) at the right side of the traces indicate the current level of the closed state. The arrowheads point to an infrequent substate. Solutions were: Bath: 120 mM potassium glutamate, 2 mM EGTA, 4.42 mM $CaCl_2$, 2.27 mM $MgCl_2$, 2 mM MgATP, 10 mM Tris (pH 7.2, adjusted with Mes; free Ca^{2+} = 150 nM, free Mg^{2+} = 2 mM). Pipette: 10 mM KCl, 2 mM $MgCl_2$, 1 mM $CaCl_2$, 2 mM Hepes (pH 5.8, adjusted with BTP). b, From a holding potential of 30 mV in intervals of 1.1 s, the current-voltage relation of an open NORC channel was recorded by imposing a voltage ramp on an inside-out patch (same experiment as shown in a). From a holding potential of 30 mV, voltage ramps were applied in intervals of 1.1 s. For further details on the procedure, see text. c, Voltage dependence of the open probability of NORC in the same inside-out patch at 150 nM (○) and 5 μM (●) Ca^{2+} (buffered with 2 mM HEDTA) in the bath. Data obtained at both Ca^{2+} concentrations were pooled and fitted with the following Boltzmann equation:

$$p_0 = \frac{P_{0,max}}{1 + \exp[\delta F(U_{1/2} - U)/RT]}$$

where $P_{0,max}$ is the maximal open probability, δ is the apparent minimal gating charge, $U_{1/2}$ is the voltage at which p_o is 0.5, and U is the applied potential. F, Faraday's constant; R, gas constant; T, absolute temperature. Best fit of the data is represented by the solid line with $U_{1/2}$ = 3.6 mV and δ = 1.3. d. Corresponding current-voltage relations for NORC-channel activity at 150 nM (○) and 5 μM (●) Ca^{2+} reconstructed from unitary current amplitudes. Only the most frequent conductance level is shown. e, Current traces obtained by open-channel ramps (NORC) from one inside-out patch reflecting several (four) subconductance levels, under the same experimental conditions as in a. Solid line represents a description of current-voltage curves with fourth-order polynomials.

any of the ions present, but was close to the reversal potential of NORC in whole-cell experiments (Fig. 4c).

Voltage dependence and the averaged deactivation time course of putative NORC channels also showed good agreement with whole-cell data (Fig. 5c and data not shown). To determine if the correlation between the occurrence of NORC currents in whole-cell experiments and the cytoplasmic Ca^{2+} concentration was caused by direct interaction of Ca^{2+} with the channel (or another protein closely associated with it), the open probability was determined at 150 nM Ca^{2+} in the bath for a set of voltages from continuous (about 3 min) current recordings. Subsequently, the Ca^{2+} concentration was elevated to 5 μM and the patch was again challenged with a range of test potentials. As can be seen in Figure 5c, the open probability of the channel was not affected by this manipulation (and, hence, data at both Ca^{2+} concentrations were pooled for the fit). Neither was the unitary conductance of NORC channels affected by the Ca^{2+} concentration at the cytosolic face of the membrane (Fig. 5d), indicating that Ca^{2+} regulation of NORC-channel activity is indirect via a cytoplasmic factor.

To give an adequate picture of NORC-channel activity, it should be noted that there was considerable variability with respect to the conductance and open-channel current-voltage relations both in one patch and among different

experiments, indicating that several channel types contribute to NORC currents. Single channels could either be ohmic or outward rectifying (as in the experiment shown in Fig. 5, a–d). Moreover, at least four different conductance levels (14, 26, 36, and 97 pS; data from three patches) could be distinguished. Open-channel ramps obtained from a recording of this kind are superimposed in Figure 5e. Experimental conditions were identical to those for the experiment shown in Figure 5, a to d. Channel activity increased strongly with a depolarization of the membrane and the reversal potential (after leak subtraction) was −10 mV; on this basis, channels were identified as NORC. The relevance of this diversity of single-channel properties for whole-cell currents can be taken from the observation that the form of the instantaneous current-voltage relations from tail currents varied in the same way: in part of the experiments it was linear, for example, in Figure 4b, whereas in others strong outward rectification occurred (data not shown).

The Voltage Dependence of KORC Depends on the Apoplastic K^+ Concentration: Whole-Cell and Single-Channel Data

Figure 6a shows superimposed whole-cell current traces resulting from consecutive, depolarizing voltage steps at three different K^+ concentrations in the bath. Outward currents were identified as KORC currents by their voltage dependence and by the reversal potential of tail currents, which was close to E_{K+} (data not shown). Time-dependent currents, normalized to the protoplast surface, are plotted as a function of the membrane potential in Figure 6b. The current-voltage curve shifted to more positive potentials when the K^+ concentration in the bath was increased, roughly following the equilibrium potential for K^+. This effect was specific for K^+. Adding NMG to the bath did not alter the voltage dependence of the gate (data not shown), indicating that modulation of gating was not caused by a nonspecific parameter such as ion strength.

Properties of single KORC channels were analyzed by making use of the cell-attached, inside-out, and outside-out patch configuration. In Figure 7a, current traces from an inside-out patch responding to a pulse protocol (as shown on top of the current traces) are superimposed. Channel activity increased with depolarization of the patch. Conspicuously, when the membrane was stepped to a potential that induces channel closure, rapid flickering between an open and closed state was observed before the channel closed definitely (see enlarged trace, bottom of Fig. 7a).

A similar kind of behavior was previously reported for K^+-selective, depolarization-activated channels in *Amaranthus tricolor* shoot cells (Terry et al., 1991) and two *Plantago* species (Vogelzang and Prins, 1994). Single-channel current levels were extracted from amplitude histograms and plotted versus the applied voltage to obtain the single-channel current-voltage relation as shown in Figure 7b. The unitary conductance of KORC at the reversal potential was 11.1 ± 2.7 pS at 120 mM K^+ at the cytoplasmic face of the membrane and 1 mM K^+ on the outside (mean value ± SD; n = 4), 19.6 ± 2.9 pS at 120/10 mM K^+ (n = 7), and 24 pS at 120/30 mM K^+ (n = 2). For the experiment shown in Figure 7b, a conductance of 21 pS was determined.

Single KORC channels and whole-cell currents also showed similar voltage dependence (Fig. 7c). In one inside-

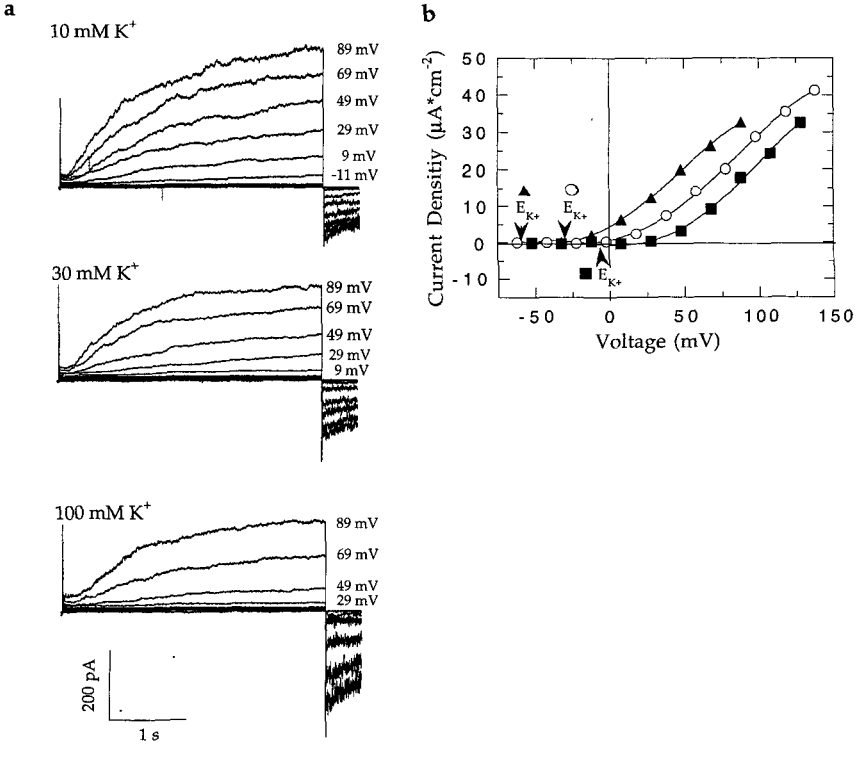

Figure 6. Dependence of KORC on the external K^+ concentration. a, Whole-cell KORC currents (superimposed traces) at 10, 30, and 100 mM KCl in the bath. The holding potential was −101 mV. Solutions were: Bath: 10, 30, or 100 mM KCl, 1 mM $CaCl_2$, 2 mM $MgCl_2$, 10 mM Hepes, pH 5.8, adjusted with Mes. Pipette: 112 mM potassium glutamate, 8 mM KOH, 2 mM HEDTA, 30 µM calcium gluconate, 1.75 mM $MgCl_2$ (1.5 µM free Ca^{2+}, 2 mM free Mg^{2+}), 10 mM Hepes, pH 7.2, adjusted with BTP. b, Current-voltage plots derived from the traces shown in a. Current densities were calculated after subtracting the instantaneous "leak." External solution: 10 mM (▲) K^+ (E_{K+} = −60 mV), 30 mM (○) K^+ (E_{K+} = −34 mV), and 100 mM (■) K^+ (E_{K+} = −4 mV).

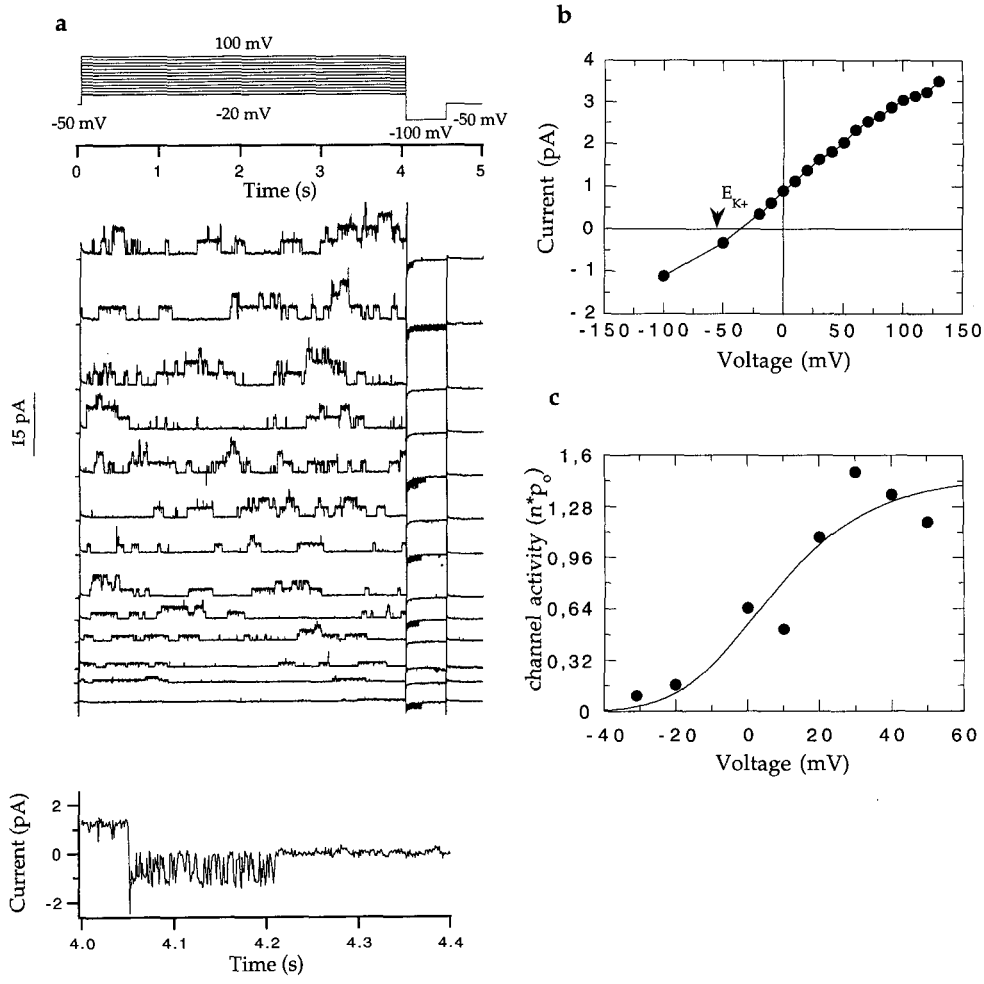

Figure 7. Properties of single KORC channels. a, Superimposed current traces recorded on an inside-out patch with KORC-channel activity. Voltage protocol was as indicated above the traces (in increments of 10 mV). Below, rapid flickering of the channel after repolarization to −100 mV is shown on an enlarged scale. Solutions were: Bath: 109 mM potassium glutamate, 11 mM KOH, 0.9 mM calcium gluconate, 1.95 mM $MgCl_2$, 2 mM EGTA, 10 mM Hepes, 2 mM MgATP (150 nM free Ca^{2+}, 2 mM free $MgCl_2$), pH 7.2 (Mes). Pipette: 10 mM KCl, 1 mM $CaCl_2$, 2 mM $MgCl_2$,10 mM Hepes, pH 5.8 (BTP). Data were filtered at 0.5 kHz and sampled at 2 kHz. b, Current-voltage relation of unitary KORC current derived from the experiment shown in a. c, Voltage dependence of KORC-channel activity (n^*p_o). The channel activity was calculated according to:

$$\sum_{n=1}^{a} n \times t_n$$

where n = number of channels that were open simultaneously; t_n = fraction of time in which n channels are open simultaneously; and a = maximal number of channels observed simultaneously. Data were fitted with the following Boltzmann equation:

$$n^*p_0 = \frac{n^*p_{0,\max}}{(1 + \exp[\delta F(U_{1/2} - U)/RT])^4}$$

where $n^*p_{o,max}$ is the maximal channel activity. For other symbols, see legend to Figure 5c. Best fit (solid line) was obtained with $n^*p_{o,max}$ = 1.47 (±0.31), δ = 3.4 (±1.97), and $U_{1/2}$ = −22 (±12) mV (numbers in parentheses, error of estimate of the fit). Quality of the fit: r = 0.94. Solutions as in a.

out patch clamped for 5 min at each conditioning voltage, channel activity could be quantified as the product of the number of channels in the patch and the open probability (n^*p_o). Channel activity increased with a depolarization of the patch. The voltage dependence could be fitted with a Boltzmann function (see legend to Fig. 7), corresponding to a Hodgkin-Huxley model with four identical, independent gates. This model was based on a quantitative analysis of

whole-cell KORC currents (Wegner, 1996; L.H. Wegner and A.H. DeBoer, unpublished data). Fit parameters for whole-cell and single-channel experiments agreed well (data not shown). Often, channel activity fluctuated unpredictably during an experiment, precluding a quantitative analysis of gating. Qualitatively, activity was always higher at more positive potentials. Like NORC, single KORC-channel activity in the inside-out configuration was not sensitive to an increase in cytosolic Ca^{2+} (data not shown).

Selectivity of KORC

Further experimentation on the selectivity of KORC was undertaken on both whole-cell currents using the tail-current method (see Fig. 8a) and on single-channel recordings on excised patches by imposing ramp protocols (see explanations given for NORC single-channel measurements). Similar values for reversal potentials were determined in both configurations at different K^+ gradients, further corroborating that whole-cell and unitary currents resulted from activity of the same channel (Fig. 8b). Reversal potentials positive of E_{K+} confirm earlier observations that KORC currents are not carried exclusively by K^+. To determine whether KORC is Ca^{2+} permeable, the reversal potential of KORC channels was determined after removing Ca^{2+} from the bath and substituting 2 mM EGTA. Indeed, current ramps reversed exactly at E_{K+}, as shown in Figure 8c. Based on these data, the relative permeability of KORC for Ca^{2+} over K^+ could be calculated using a modified version of the Goldman equation (Lewis, 1979):

$$\frac{P_{Ca^{2+}}}{P_{K^+}} = \frac{[K]_0 - [K]_i 10^{U/59mV}}{4\left(\frac{10^{U/59mV}}{1 + 10^{U/59mV}}[Ca^{2+}]_i - \frac{1}{1 \times 10^{U/59mV}}[Ca^{2+}]_0\right)} \quad (2)$$

The calculated value was 0.68 with 1 mM K^+ and Ca^{2+} in the bath. This should be considered an approximation, because the Goldman equation is based on independent diffusion of ions in a constant electrical field, a prerequisite that is clearly not met by permeation through KORC, as inferred from single-channel properties.

From a physiological point of view, the ability of KORC to transport Na^+ was of special interest, and was investigated on inside-out patches. The membrane was first exposed to 120 mM K^+ in the bath with 30 mM K^+ in the pipette, and the patch was challenged with a ramp protocol (Fig. 8d; see legend for details). Subsequently, K^+ was substituted for Na^+, and the experiment was repeated. In Figure 8d, single-ramp currents and averaged traces with K^+ and Na^+ on the cytosolic side of the membrane are shown. Before averaging traces, current levels representing the closed state had to be removed because channels underwent rapid flickering, especially when the direction of the current was inward. Note that no outward current was seen with Na^+ on the cytosolic side, indicating that KORC was virtually Na^+ impermeable. Inward currents (carried by K^+ in the pipette solution), on the other hand, were generally unaffected. It seems that internal Na^+ has no blocking effect on the channel.

Perfusion Experiments on Intact Seedlings

To test the hypothesis that K^+ release to the xylem is mediated by KORC, we perfused xylem vessels of intact seedlings with the K^+-channel blocker TEA, which was previously shown to inhibit the K^+ outward rectifier (Wegner and Raschke, 1994). Perfused roots from seedlings grown under low-salt conditions were allowed to take up K^+ from an external medium. We perfused the xylem vessels with the blocker at a concentration of 50 mM, as required for an effective blockage of the channel. Control seedlings were perfused with 50 mM NMG, an organic cation that does not affect channel activity. As shown in Figure 9, TEA blocked K^+ transport to the shoot almost completely. The background level of K^+ was measured from reference seedlings that were not exposed to K^+ during the experiment; in these plants, the K^+ content of the shoot was about 60% of that found in seedlings treated with K^+ and perfused with NMG, when the rest of the caryopsis was removed from 3-d-old seedlings. Note that K^+ uptake into root tissue was higher in plants perfused with TEA than in those perfused with NMG, suggesting that the inhibition of K^+ supply to the shoot by TEA was not caused by a blockage of K^+ uptake by the root, but by a selective inhibition of K^+ release to the xylem. Perfusion with 20 mM Ba^{2+}, another K^+-channel blocker, was largely ineffective (data not shown), in analogy to guard cells (Kelly et al., 1995).

DISCUSSION

Evidence for Two Depolarization-Activated Outward Rectifiers Coexisting in the Plasma Membrane of XPCs and the Role of Ca^{2+}

In XPCs, two distinct types of outward rectifiers, KORC and NORC, have been recorded. We have shown here that the cytosolic free Ca^{2+} concentration imposed by a defined Ca^{2+} level in the pipette solution has a strong bearing on the probability with which either KORC or NORC are observed in whole-cell recordings (Fig. 2b). This provides evidence for the capability of the plasma membrane to switch between two conductance states with the cytosolic free Ca^{2+} concentration working as a trigger; it implies the presence of both KORC and NORC channels in the plasma membrane of the majority of the protoplasts. Cytosolic Ca^{2+} does not seem to interact with the channel protein directly, as indicated by the absence of any Ca^{2+} effect on single NORC (Fig. 5, c and d) or KORC channels.

In inside-out patches with 150 nM free Ca^{2+} in the bath, KORC and NORC channel activities were observed with about the same frequency. The occurrence of either conductance was probably related to the Ca^{2+} status of the protoplast before the excision of the patch. Inside-out patches were excised after the cell-attached configuration had been established; under these conditions, the Ca^{2+} concentration inside the cell was not under experimental

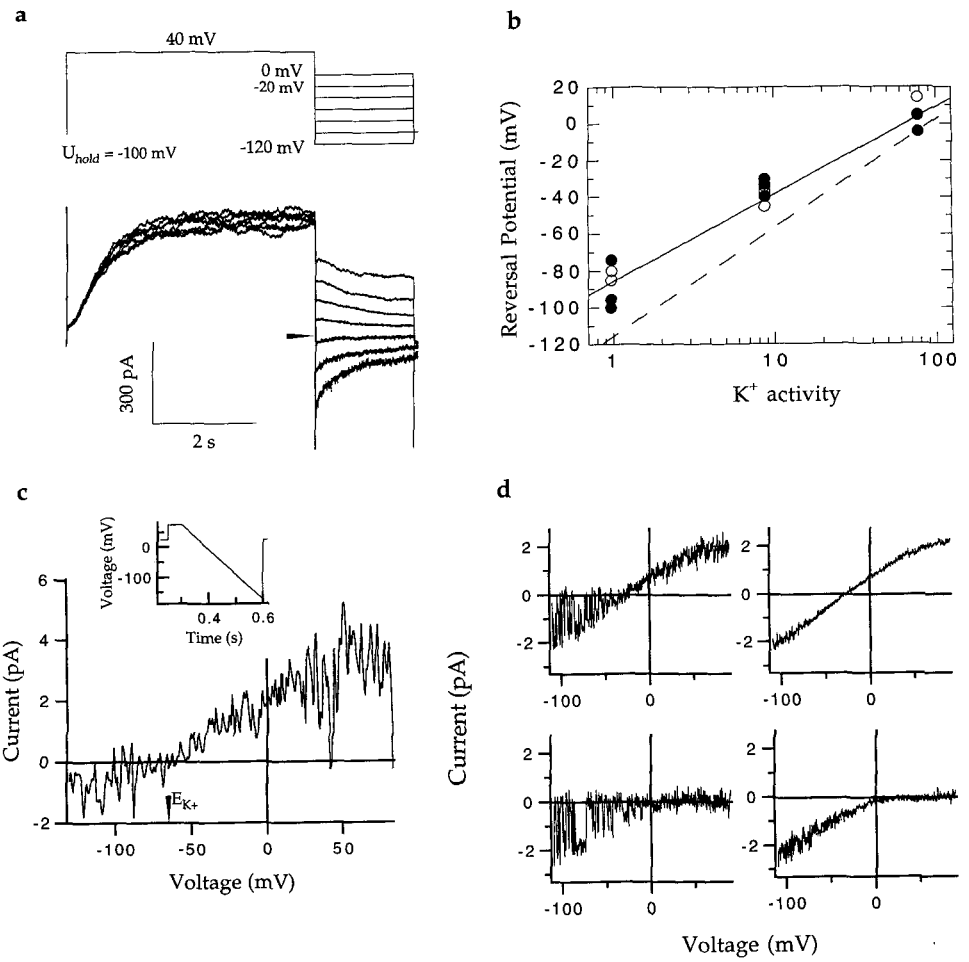

Figure 8. Selectivity of KORC. a, Tail-current experiment on KORC in the whole-cell configuration to determine the reversal potential (see pulse protocol on top). Solutions were: Bath: 1 mM KCl, 2 mM $MgCl_2$, 1 mM $CaCl_2$, 2 mM Hepes, pH 5.8, adjusted with BTP. Pipette: 120 mM KCl, 10 mM EGTA, 4.42 mM $CaCl_2$, 2.27 mM $MgCl_2$, 2 mM MgATP, 10 mM Tris, pH 7.2, adjusted with Mes; free Ca^{2+} = 150 nM, free Mg^{2+} = 2 mM. The arrowhead indicates where the tail currents reverse. b, Dependence of reversal potentials of KORC currents on the activity of K^+ in the bath. The K^+ activity in the pipette was 91 mM for all experiments. Reversal potentials were determined by tail current analysis in the whole-cell configuration (●) or by imposing voltage ramps on open channels in excised patches (○). The reversal potential shifted by 43 mV per 10-fold increase in the external K^+ activity (solid line). The dotted line marks the Nernst potential for K^+. In all experiments, 1 mM Ca^{2+} was present on the apoplastic side and 150 nM free Ca^{2+} was present on the cytosolic side. c, Current through a single KORC channel in the outside-out configuration elicited by a voltage ramp with no Ca^{2+} and 2 mM EGTA in the bath (see inset for voltage protocol). There was 120 mM K^+ in the pipette and 10 mM in the bath (for further details on the solutions, see a; note that the bath and pipette solution were exchanged). Note that $E_{rev} = E_{K+}$. In the control experiment with 1 mM Ca^{2+} and no EGTA in the bath, E_{rev} was −40 mV (not shown). d, Current-voltage curves from open-channel ramps in the inside-out configuration. The patch was kept at 100 mV; 200-ms voltage ramps were applied ranging from 100 to −100 mV. These ramps were imposed every 2 s. The top figures show ramps with 120 mM K^+ on the bath side (cytosolic side), single recording (left; note open-channel flickering) and average of 15 traces (right; before averaging the traces, closed-state currents were removed). The two figures below depict ramps that were recorded after K^+ had been replaced by Na^+ in the bath. Again, single current-voltage sweep on the left and average of 11 traces on the right. Solutions were: Pipette: 30 mM KCl, 1 mM $CaCl_2$, 2 mM $MgCl_2$, 10 mM Hepes, pH 5.8, adjusted with Mes. Bath: 112 mM potassium glutamate or sodium glutamate, 8 mM KOH or NaOH, respectively, 2 mM HEDTA, 30 μM calcium gluconate, 1.75 mM $MgCl_2$ (1.5 μM free Ca^{2+}, 2 mM free Mg^{2+}), 10 mM Hepes, pH 7.2, adjusted with BTP.

control. This was different in outside-out patches that were formed following the whole-cell configuration. Here, KORC and NORC single channels were observed only when the whole-cell configuration had been established with 150 nM and 5 μM Ca^{2+} in the pipette, respectively. These experiments suggest that the status of the membrane in the whole cell is conserved after patch excision. The missing link may be a Ca^{2+}-dependent kinase (or phosphatase) that regulates the activity of KORC and NORC channels. Ca^{2+}-dependent kinases are indeed associated with the plasma membrane of monocot root cells (Schaller et al., 1992).

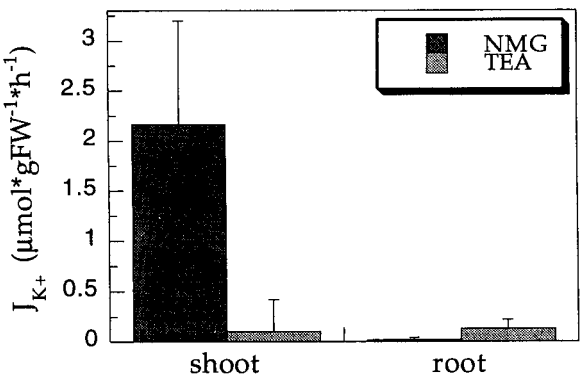

Figure 9. K^+ transport to the shoot is inhibited in barley seedlings perfused with TEA. Transport was calculated from the K^+ content of root and shoot tissue, respectively, according to:

$$J_{K^+} = \frac{([K^+]_x - [K^+]_{ref}) \times gDW_x}{36h \times gFW_r}$$

where $[K^+]_x$ is the K^+ content of shoot or root (μmol/g dry weight) for treatments with 5 mM K^+ in chamber B (either perfused with TEA or NMG); gFW_r is the fresh weight of the root; and $[K^+]_{ref}$ is the K^+ content of reference seedlings (without K^+ added to solution in chamber B). Mean values ± SE are shown for five experiments. DW, Dry weight; FW, fresh weight.

Physiological Implications of NORC Activation

Activation of NORC in XPCs has two closely associated effects: a depolarization to about 0 mV and a massive efflux of salts at a wide range of ionic relations in the cell and in the xylem. (Note that in the case of NORC, the current amplitude gives no direct indication of net salt fluxes because it only reflects the imbalance of cation and anion movement.) Activation of NORC would tend to dissipate ionic gradients across the membrane and, because the chemical gradient of the relevant ions is downhill from the cytosol to the xylem sap, ions would flow into the xylem lumen upon NORC activation. This may be functional in two respects: (a) Na^+ loading: NORC may operate as an nonspecific pathway for salt release to the xylem sap. It must be kept in mind, however, that NORC activity is restricted to high concentrations of cytosolic Ca^{2+}, indicating that it is confined to situations such as stress. Support for a role of NORC in xylem loading comes from the observation that it conducts Na^+ as well as K^+ (Wegner and Raschke, 1994), whereas KORC seems to be impermeable to Na^+ (see Fig. 8d). Barley is known to be a "Na^+ includer," i.e. it transports Na^+ to the shoot in considerable amounts (Lynch and Läuchli, 1984, and refs. therein). Xylem loading of Na^+ could therefore require functioning of NORC. (b) Signaling: NORC has properties that may be associated with a role in long-distance signaling. First, Ca^{2+}-induced activation of NORC will rapidly depolarize the cell to about 0 mV. This strong depolarization is largely unaffected by the ionic gradients across the membrane because the reversal potential of NORC is almost independent of the ionic composition of the solutions on both sides of the membrane (see Fig. 4c). Second, salt release from XPCs to the xylem through NORC would be accompanied by a massive water efflux (and a turgor breakdown of the cell), giving rise to a local increase of pressure in the xylem that can propagate through the vessel (Malone, 1994). This means that NORC can be involved in the transduction of a combined electrical and hydraulic signal.

Physiological Implications of KORC Activation

In analogy to guard cells, KORC is supposed to mediate K^+ release from XPCs, provided that an anion conductance operates simultaneously (Wegner and Raschke, 1994). Perfusion data on intact seedlings with the K^+-channel blocker TEA support this hypothesis (Fig. 9). Note that TEA does not affect NORC. Sustained K^+ efflux through KORC requires a low free Ca^{2+} concentration in XPCs. Because KORC discriminates poorly against Ca^{2+}, KORC activation can result in a Ca^{2+} influx. This may inactivate KORC channels and activate NORC, unless the Ca^{2+} gradient is maintained by pumping Ca^{2+} out of the cell (Bush, 1993). Our flux data indicate that KORC indeed mediates most of the K^+ flux to the xylem, suggesting that some mechanism exists to stabilize KORC activity by keeping cellular Ca^{2+} at a low level.

A Model for the Regulation of K^+ Transport to the Xylem by Shoot Demand

The release of K^+ to the xylem is tightly regulated by the demand for this ion in the shoot, i.e. by the growth rate and the salt status of the plant, as shown by different experimental approaches (Drew et al., 1990; Engels and Marschner, 1992; see also the introduction). This feedback control indicates that K^+ efflux from XPCs in the root is adjusted by a signal coming from the shoot. Using split-root experiments, Drew et al. (1990) obtained conclusive evidence that the amount of K^+ recirculated via the phloem served as a signal for K^+ demand of the shoot (Fig. 10a). It is well known that K^+ circulates in plants and that transfer of this ion from the phloem to the xylem occurs in roots (Jeschke et al., 1985; Wolf and Jeschke, 1987). In salt-stressed barley, Wolf and Jeschke (1987) found that at least 40% of K^+ transported to the shoot is retranslocated to the root via the phloem. Considering the data of Drew et al. (1990), it seems that this percentage is much higher under their conditions. Little is known yet about the mechanism and pathway of K^+ delivery from the phloem to the xylem. Drew and co-workers (1990) propose a symplastic transport from sieve elements to XPCs, followed by a release to the xylem vessels.

We consider it more likely that K^+ is released by the phloem into the apoplast of the stele that is in connection with the xylem sap. In this scenario, the apoplastic K^+ concentration, closely linked to the K^+ concentration in the phloem, is the "signal" sensed by the XPCs that regulates K^+ release by these cells into the vessels (Fig. 10). Aspects of K^+ circulation and homeostasis have been brought into perspective in a review by Kochian and Lucas (1988). Summarizing earlier work on this topic, they stated that "since a large portion of K^+ moving in the xylem transpiration stream is supplied by the phloem, the concept gains

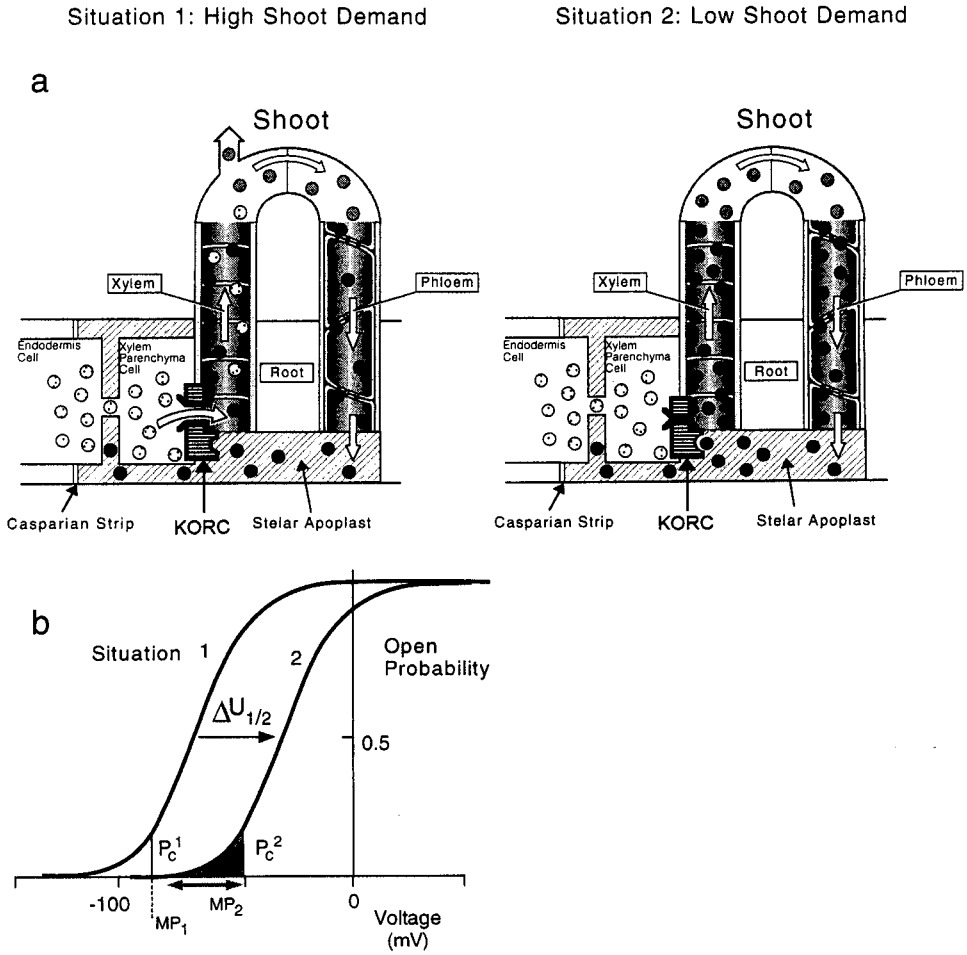

Figure 10. A model for the role of KORC in maintaining K^+ homeostasis in barley. a, Schematic diagrams showing the pathways of long-distance transport of K^+ in plants and the role of the XPCs in regulating the supply of K^+ to the shoot. K^+ ions moving upward in the xylem can either emanate from the phloem (●) or move into the xylem sap after being released by the xylem parenchyma (dotted circles). According to this model a large fraction of K^+ is circulating in the plant via phloem and xylem, and only a small fraction in the transpiration stream is retrieved via the xylem parenchyma from the K^+ pool in the cortex, the site of K^+ uptake from the soil. The diagram on the left side (situation 1) represents a situation of high shoot demand or K^+ deficiency, which is reflected in a low apoplastic K^+ concentration and high radial K^+ flux to the xylem. In contrast, the right diagram shows a situation of low shoot demand and full supply of K^+ (situation 2). The K^+ concentration in the phloem and, subsequently, in the stelar apoplast is high, resulting in a low radial flux of K^+ into the xylem vessels. The apoplastic K^+ concentration, channel activity of KORC, and the free-running membrane potential of XPCs interact in a complex way, as shown in b. In a schematic plot, the voltage dependence of the channel activity is shown in a situation of a low (situation 1) and high (situation 2) apoplastic K^+ concentration. An elevation of apoplastic K^+ results in a shift of the current-voltage curve to more positive potentials (Δ^U) expressed in terms of the open probability of the channel (see arrow). Two scenarios are feasible: (a) $MP_2 - MP_1 = \Delta^U$. If the membrane potential follows $\Delta^U{}_{1/2}$ exactly, channel activity and therefore K^+ efflux will not be affected. (b) $MP_2 - MP_1 < \Delta^U$. If the membrane potential shifts less than Δ^U or remains unchanged, the amplitude of KORC current will decrease, and K^+ efflux across the plasma membrane of XPCs will be reduced. The latter situation will occur if other conductances such as pump currents or anion currents, which are generally unaffected by external K^+, exert control on the membrane potential as well.

strength that K^+ transfer, from the phloem, influences the ionic environment of the root xylem parenchyma." It should be noted that an effective isolation of the apoplastic K^+ pool in the stele from that in the cortex is an important prerequisite for the model presented here; there is good experimental evidence for the Casparian band in the endodermal cell layer to form such an apoplastic transport barrier (for review, see Clarkson, 1993). In summary, our present view on K^+ homeostasis in plants (Fig. 10a), following that of Kochian and Lucas (1988) and Drew et al. (1990), is that K^+ is circulating in the plant via xylem and phloem and K^+ that is removed from this continuous circle in the shoot, e.g. in growing tissues (Wegner et al., 1994), is replenished in the root by K^+ release from XPCs.

To study the molecular mechanism of K^+ efflux control from XPCs by apoplastic K^+, we recorded KORC currents at various K^+ concentrations in the bath. Channel gating responds to changes in the apoplastic K^+ concentration,

leading to a shift in the current-voltage relation that roughly follows E_{K+}, as was previously shown for guard cells (Schroeder, 1988). An increase in the apoplastic K^+ concentration will result in a reduction of K^+ efflux if the membrane potential is unaffected or, more realistically, if the shift in the potential is smaller than the shift of the current-voltage relation for KORC (Fig. 10b; see legend for a more detailed explanation).

The voltage dependence of KORC is expressed in terms of the open probability of the channel (compare Fig. 7c). A more detailed quantitative analysis of the dependence of KORC on apoplastic K^+ will be given in a forthcoming paper (L.H. Wegner and A.H. De Boer, unpublished data; see also Wegner, 1996). Most likely, hormonal signaling and transpiration, among other factors, will interfere with whole-plant K^+ transport. Under field conditions, the role of recirculated K^+ on radial transport of K^+ to the stele may be less clear than under the experimental conditions carefully designed by Drew et al. (1990).

ACKNOWLEDGMENTS

We thank R.A. Boekman (Department of Plant Ecology, Vrije Universiteit Amsterdam, The Netherlands) for assistance with flame photometry; Dr. David Clarkson (Long Ashton Research Station, Bristol, UK) for discussion; and S. Vogelzang (Vrije Universiteit Amsterdam, Amsterdam, The Netherlands) for critically reading the manuscript.

Received May 16, 1997; accepted September 8, 1997.

LITERATURE CITED

Bush DS (1993) Regulation of cytosolic calcium in plants. Plant Physiol **103:** 7–13

Canny MJ (1995) A new theory for the ascent of the sap: cohesion supported by tissue pressure. Ann Bot **75:** 343–357

Clarkson DT (1993) Roots and the delivery of solutes to the xylem. Philos Trans R Soc Lond Ser B **341:** 5–17

De Boer AH, Wegner LH (1997) Regulatory mechanisms of ion channels in xylem parenchyma cells. J Exp Bot **48:** 441–449

Drew MC, Saker LR (1984) Uptake and long distance transport of phosphate, potassium and chloride in relation to internal ion concentrations in barley: evidence of non-allosteric regulation. Planta **160:** 500–507

Drew MC, Webb J, Saker LR (1990) Regulation of K^+ uptake and transport to the xylem in barley roots: K^+ distribution determined by electron probe X-ray microanalysis of frozen-hydrated cells. J Exp Bot **41:** 815–825

Engels C, Marschner H (1992) Adaption of potassium translocation into the shoot of maize (*Zea mays*) to shoot demand: evidence for xylem loading as a regulating step. Physiol Plant **86:** 263–268

Führ KJ, Warchol W, Gratzl M (1993) Calculation and control of free divalent cations in solutions used for membrane studies. Methods Enzymol **221:** 149–157

Hamill O, Marty A, Neher E, Sakmann B, Sigworth FJ (1981) Improved patch-clamp techniques for high-resolution current recordings from cells and cell-free membrane patches. Pfluegers Arch **391:** 85–100

Jeschke WD, Atkins CA, Pate JS (1985) Ion circulation via phloem and xylem between root and shoot of nodulated white lupin. J Plant Physiol **117:** 319–330

Kelly WB, Esser J, Schroeder JI (1995) Effects of cytosolic Ca^{2+} and limited, possible dual, effects of G protein modulators on guard cell inward potassium channels. Plant J **8:** 479–489

Kochian LV, Lucas WJ (1988) Potassium transport in roots. Adv Bot Res **15:** 93–178

Lewis CA (1979) Ion-concentration dependence of the reversal potential and the single channel conductance of ion channels at the frog neuromuscular junction. J Physiol **286:** 417–445

Lynch J, Läuchli A (1984) Potassium transport in salt stressed barley roots. Planta **161:** 295–301

Malone M (1994) Wound-induced hydraulic signals and stimulus transmission in *Mimosa pudica* L. New Phytol **128:** 49–56

Neher E (1992) Corrections for liquid junction potentials in patch clamp experiments. Methods Enzymol **207:** 123–130

Roberts SK, Tester M (1995) Inward and outward K^+-selective currents in the plasma membrane of protoplasts from maize root cortex and stele. Plant J **8:** 811–825

Robinson RA, Stokes RM (1968) The Debye-Hückel formula for the activity coefficient. *In* Electrolyte Solutions. Butterworth, London, pp 229–232

Schaller GE, Harmon AC, Sussman MR (1992) Characterization of a calcium- and lipid-dependent protein kinase associated with the plasma membrane of oat. Biochemistry **31:** 1721–1727

Schroeder JI (1988) K^+ transport properties of K^+ channels in the plasma membrane of *Vicia faba* guard cells. J Gen Physiol **92:** 667–683

Terry BR, Tyerman SD, Findlay GP (1991) Ion channels in the plasma membrane of *Amaranthus* protoplasts: one cation and one anion channel dominate the conductance. J Membr Biol **121:** 223–236

Vogelzang SA, Prins HBA (1994) Patch clamp analysis of the dominant plasma membrane K^+ channel in root cell protoplasts of *Plantago media* L.: its significance for the P and K state. J Membr Biol **141:** 113–122

Ward JM, Schroeder JI (1994) Ca^{2+}-activated vacuolar K^+ channels and Ca^{2+} induced Ca^{2+} release by slow vacuolar channels implicated in stomatal closing. Plant Cell **6:** 669–689

Wegner LH (1996) The role of ion channels in salt transport between the xylem and adjacent cells. PhD thesis. Vrije Universiteit, Amsterdam, The Netherlands

Wegner LH, De Boer AH, Raschke K (1994) Properties of the K^+ inward rectifier in the plasma membrane of xylem parenchyma cells from barley roots: effects of TEA^+, Ca^{2+}, Ba^{2+} and La^{3+}. J Membr Biol **142:** 363–379

Wegner LH, Raschke K (1994) Ion channels in the xylem parenchyma of barley roots. A procedure to isolate protoplasts from this tissue and a patch-clamp exploration of salt passageways into xylem vessels. Plant Physiol **105:** 799–813

Wolf O, Jeschke WD (1987) Modeling of sodium and potassium flows via phloem and xylem in the shoot of salt-stressed barley. J Plant Physiol **128:** 371–386

Zimmermann U, Meinzer FC, Benkert R, Zhu JJ, Schneider H, Goldstein G, Kuchenbrodt E, Haase A (1994) Xylem water transport: is the available evidence consistent with the cohesion theory? Plant Cell Environ **17:** 1169–1181